Millimeter-Wave Amplification by Resonance Saturation*

BENJAMIN SENITZKY, GORDON GOULD, AND SYLVEN CUTLER
TRG, Incorporated, Syosset, New York

(Received 3 October 1962; revised manuscript received 6 February 1963)

The nonlinear properties of a power-saturated resonant medium are used to obtain amplification of millimeter-wave radiation. Experiments demonstrating this effect are performed with the 3.5-mm rotational resonance of hydrogen cyanide ($HC^{12}N^{15}$) gas. An incoming radiation spectrum consisting of a strong saturating component at 3.5 mm and weak sidebands is transmitted through a gas-filled, $\frac{3}{4}$-in.-diam, 20-ft circular waveguide operated in the TE_{01} mode. Under certain conditions power can be transferred from the strong saturating component to the weak sidebands. A sideband gain with a maximum value of 1.5 dB is measured when the sidebands are phased for amplitude modulation and the saturating component input power is 4.8 mW. The bandwidth for this type of amplification is equal to the power-broadened linewidth. Sidebands phased for frequency modulation are always attenuated. The experimental results are in agreement with computations based on the solution of the quantum-mechanical Boltzmann equation. These computations indicate that a single sideband can also be amplified.

I. INTRODUCTION

WE have studied the response of resonant media to a millimeter-wave radiation spectrum consisting of a strong Fourier component at the resonance frequency and weak sidebands. The absorption of the sidebands will depend on the amplitude and phase of the strong component if: (a) The latter appreciably changes the equilibrium population distribution and (b) the frequency difference between the strong component and the sidebands is not greater than the power-broadened linewidth. We have found that, under certain conditions, the absorption of the sidebands can decrease through zero and become an amplification. Thus, if the strong (saturating) component and the weak sidebands are simultaneously transmitted through the medium, the saturating component will be attenuated and the sidebands will be amplified. We have observed this effect at 3.7-mm wavelength in a crystalline solid (Fe^{3+}-doped TiO_2)[1] exhibiting an electron paramagnetic resonance spectrum and at 3.5-mm wavelength in a molecular gas ($HC^{12}N^{15}$) exhibiting a rotational resonance spectrum. This article is primarily concerned with the theoretical description and experimental verification of this effect in the gas.

II. THEORY

The problem of collision-broadened absorption of monochromatic radiation has been considered by Karplus and Schwinger.[2] These authors computed the induced molecular dipole moment by solving the quantum-mechanical Boltzmann equation for the density matrix. We will follow their procedure but use a different electromagnetic field perturbation. Our problem here is to find the frequency spectrum of a dipole moment induced by a field consisting of a strong saturating component and weak sidebands. We will first solve the Boltzmann equation (to first order in the sideband fields) when the frequency separations of the saturating component and sidebands are much less than the molecular collision frequency. The effect of the medium on the radiation can then be determined by comparing the induced dipole moment spectrum with the applied field spectrum. The conditions under which the medium can amplify power at the sideband frequencies will be found and the characteristics of this amplification will be further investigated when the restriction on the frequency separations of the saturating component and sidebands is removed.

The Hamiltonian of the gas molecule, including the perturbation, $V(t)$, of the external field is

$$H(t)=H_0-\mathbf{p}\cdot\mathbf{F}(t)=H_0+V(t), \tag{1}$$

where H_0 is the Hamiltonian of the isolated molecule, $\mathbf{p}$ is the dipole moment operator, and $\mathbf{F}(t)$ is the applied electric field. Using a representation in which H_0 is diagonal and introducing a "collision-averaged" density matrix, $\bar{\rho}(t)$, Karplus and Schwinger[2] write the Boltzmann equation in the following form:

$$\begin{aligned}(\partial/\partial t+i\omega_{mn}+1/\tau)\bar{\rho}_{mn}(t)&\\ =-(i/\hbar)\textstyle\sum_k[V_{mk}(t)\bar{\rho}_{kn}(t)-\bar{\rho}_{mk}(t)V_{kn}(t)]&\\ -(1/\tau)\rho_m^{(0)}\delta_{mn}-(1/\tau)(\rho_m^{(0)}-\rho_n^{(0)})&\\ \times V_{mn}(t)/\hbar\omega_{mn},&\end{aligned} \tag{2}$$

where

$$\omega_{mn}=(E_m-E_n)/\hbar \tag{3}$$

is the angular frequency associated with the transition from state m to state n,

$$\rho^{(0)}=\exp(-H_0/kT)/\mathrm{Tr}[\exp(-H_0/kT)] \tag{4}$$

is the density matrix in the absence of an external field and τ is the average time between collisions. For the experimental conditions described below Eq. (2) can be simplified as follows: (a) Only two energy levels, $m=1$ and $n=2$, need be considered. (b) The diagonal matrix elements of V are zero. (c) The last term on the right-hand side of Eq. (2) is negligible. Subject to these

* Work supported by Rome Air Development Center of the Air Force Systems Command.

[1] Final Report, AF Contract 30(602)-2033. RADC number TDR-62-577 (1962) (unpublished). Available from ASTIA, Arlington Hall Station, Arlington, Virginia.

[2] R. Karplus and J. Schwinger, Phys. Rev. **73**, 1020 (1948).

conditions the equation can be rewritten in terms of the average induced dipole moment,

$$\mathbf{p}(t)=\mathrm{Tr}[\mathbf{p}\bar{\rho}(t)]=\mathbf{p}_{12}\bar{\rho}_{21}(t)+\mathbf{p}_{21}\bar{\rho}_{12}(t), \tag{5}$$

and the average population difference,

$$D(t)=\bar{\rho}_{22}(t)-\bar{\rho}_{11}(t),$$

in the form

$$\begin{aligned}&\frac{\partial^2\mathbf{p}(t)}{\partial t^2}+\frac{2}{\tau}\frac{\partial\mathbf{p}(t)}{\partial t}+(\omega_0^2+1/\tau^2)\mathbf{p}(t)\\&\qquad=2D\omega_0|p_{12}|^2\mathbf{F}(t)/\hbar,\\&\frac{dD(t)}{dt}+(1/\tau)[D(t)-D^{(0)}]\\&\qquad=-\frac{2}{\hbar\omega_0}\left[\frac{\mathbf{p}(t)}{\tau}+\frac{\partial\mathbf{p}(t)}{\partial t}\right]\cdot\mathbf{F}(t),\end{aligned} \tag{6}$$

where $D^{(0)}$ is the equilibrium population difference, p_{12} is the matrix element of the vector component of the dipole moment operator in the field direction, and ω_0 is the resonant angular frequency which is equal to ω_{12}.

Let us write the time dependence of an applied field which consists of a saturating frequency component of amplitude F_c and sidebands of amplitudes F_n, in the form

$$\begin{aligned}\mathbf{F}(t)&=F(t)\mathbf{r}_0\\&=\{F_c\cos\omega_0t+\textstyle\sum_n F_n\cos[(\omega_0+\delta_n)t+\phi_n]\}\mathbf{r}_0,\end{aligned} \tag{7}$$

where $F_n/F_c\ll1$, $\delta_n/\omega_0\ll1$, and $\mathbf{r}_0$ is a unit vector in the field direction. This expression can be rewritten in the quasi-monochromatic form of an amplitude and phase (frequency) modulated field,

$$F(t)=F_{cq}\cos(\omega_0t+\phi_q), \tag{8}$$

where

$$\begin{aligned}F_{cq}&=F_c+\textstyle\sum_n F_n\cos(\delta_nt+\phi_n),\\\phi_q&=\textstyle\sum_n(F_n/F_c)\sin(\delta_nt+\phi_n).\end{aligned} \tag{9}$$

Slow Modulation

If the amplitude of the field in Eq. (8), F_{cq}, and the phase, ϕ_q, do not change appreciably during the collisional relaxation time, τ, we can use the known monochromatic solution of Eq. (2) to write the induced dipole moment per unit volume[2]

$$\begin{aligned}\mathbf{P}(t)&=N\mathbf{p}(t)\\&=\chi_0''\mathbf{r}_0(1+|p_{12}|^2F_{cq}^2\tau^2/\hbar^2)^{-1}F_{cq}\sin(\omega_0t+\phi_q),\end{aligned} \tag{10}$$

where N is the molecular density and

$$\chi_0''=|p_{12}|^2\tau ND^{(0)}/\hbar. \tag{11}$$

The magnitude of the induced polarization can then be expressed, to first order in F_n/F_c, as

$$\begin{aligned}P(t)=\chi_0''(1+\gamma^2)^{-1}\{&F_c\sin\omega_0t\\&+(1+\gamma^2)^{-1}\textstyle\sum_n F_n\sin[(\omega_0+\delta_n)t+\phi_n]\\&-\gamma^2(1+\gamma^2)^{-1}\textstyle\sum_n F_n\sin[(\omega_0-\delta_n)t-\phi_n]\},\end{aligned} \tag{12}$$

where

$$\gamma^2=|p_{12}|^2F_c^2\tau^2/\hbar^2$$

is a saturation parameter.

We will now consider three specific forms of the applied electric field, $F(t)$, in Eq. (7). First, when only one sideband is present, we can write

$$F(t)=F_c\cos\omega_0t+F_1\cos[(\omega_0+\delta)t+\phi_1]. \tag{13}$$

The polarization can be obtained directly from Eq. (12). For negligible γ^2, the polarization shows the expected linear behavior. For $\gamma^2<1$ (but not negligible) the incipient nonlinear behavior is in agreement with the results of Tang and Statz.[3] For larger γ^2 (saturated resonance) the induced polarization at the "image sideband" frequency $(\omega_0-\delta)$ becomes significant and must be included in determining the effect of the medium on an incident plane wave with the time dependence of Eq. (13). The spatial rate of change of the various frequency components in the plane wave can be determined from the condition that the power absorbed per unit volume from each frequency component of the radiation is equal to the electric field of this component multiplied by the time derivative of the corresponding frequency component of the polarization. The resulting coupled linear differential equations can be integrated to determine the Fourier components of the field as a function of the propagation distance. The results indicate that a field at the image sideband frequency $(\omega_0-\delta)$ will be generated that can increase until both sidebands are equal in magnitude and the resultant field is amplitude modulated.

A field, $F(t)$, containing two sidebands of equal amplitude phased for frequency modulation can be written as a special case of Eq. (7),

$$\begin{aligned}F(t)=F_c\cos\omega_0t&+F_s\cos[(\omega_0+\delta)t+\phi]\\&+F_s\cos[(\omega_0-\delta)t+\pi-\phi],\end{aligned} \tag{14}$$

where we have made the following notation change:

$$F_1=F_{-1}=F_s,\quad \delta_1=-\delta_{-1}=\delta\quad\text{and}\quad\phi_1=\pi-\phi_{-1}=\phi.$$

The attenuation of the Fourier components of a plane wave with this time dependence propagating in the z direction can be expressed as

$$\frac{1}{F_c^2}\frac{dF_c^2}{dz}=\frac{1}{F_s^2}\frac{dF_s^2}{dz}=-\frac{4\pi\omega_0\chi_0''}{c(1+\gamma^2)}=-\frac{\alpha}{1+\gamma^2}, \tag{15}$$

where α is the linear absorption coefficient. In this case all the Fourier components are equally attenuated.

[3] C. L. Tang and H. Statz, Phys. Rev. **128**, 1013 (1962).

An amplitude modulated field can be written by omitting π in the argument of the last term on the right-hand side of Eq. (14). The attenuation of the saturating component of the field, F_c, is

$$\frac{1}{F_c^2}\frac{dF_c^2}{dz}=-\frac{\alpha}{1+\gamma^2}, \tag{16}$$

but the attenuation or gain of the sidebands at the frequency $(\omega_0\pm\delta)$ will be

$$\frac{1}{F_s^2}\frac{dF_s^2}{dz}=\frac{\alpha(\gamma^2-1)}{(\gamma^2+1)^2}. \tag{17}$$

In this case the saturating component field is attenuated in the usual manner but both sideband fields, F_s, exhibit an identical power gain when $\gamma^2>1$. In the limit as the medium becomes strongly saturated and γ^2 becomes much greater than one,

$$d(F_cF_s)/dz=0, \tag{18}$$

and the sideband gain becomes equal to the saturating component attenuation.

The nonlinear behavior described above is due to the disturbance of the equilibrium population distribution by the radiation field. The power absorbed from the radiation is proportional to the product of the field intensity and the nonequilibrium population distribution. If the population distribution is changing in time, the various Fourier components of the radiation will not be absorbed equally. Thus, when the field is frequency modulated, the population difference remains constant and all Fourier components are equally absorbed; but when the field is amplitude modulated and the population difference is changing in time, the behavior of the various frequency components is distinctly different—the saturating component is attenuated and the sidebands are amplified.

Rapid Modulation

We will now use Eq. (6) to compute the polarization induced by an amplitude modulated field when the modulation frequency, δ, is *not* small compared to the collision frequency, τ^{-1}. The polarization and population difference can be expressed as a sum of frequency components

$$P(t)=\mathrm{Re}\sum_{m=-\infty}^{\infty}P_me^{-i(\omega_0+m\delta)t},$$
$$D(t)=\mathrm{Re}\sum_{m=-\infty}^{\infty}D_me^{-im\delta t}, \tag{19}$$

where nonresonant terms have been neglected. Terms involving the second or higher harmonic of the modulation frequency, δ, can be shown to be second or higher order in F_s/F_c and can also be neglected. Finally, neglecting antiresonant terms we can write the polarization as

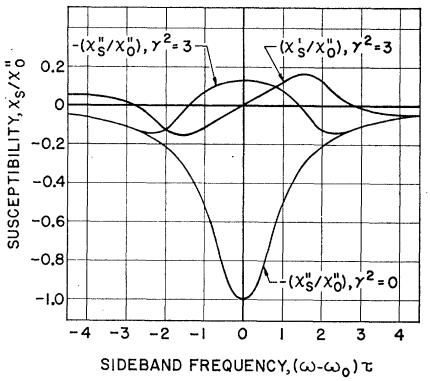

FIG. 1. Sideband susceptibilities, χ_s' and χ_s'', as a function of the frequency, $(\omega-\omega_0)\tau$, for an amplitude modulated field. Dispersion characteristics for a saturated ($\gamma^2=3$) and unsaturated ($\gamma^2=0$) resonance are shown.

$$P(t)=\mathrm{Re}\{\chi_cF_ce^{-i\omega_0t}+\chi_s^+F_se^{-i[(\omega_0+\delta)t+\phi]}+\chi_s^-F_se^{-i[(\omega_0-\delta)t-\phi]}\}, \tag{20}$$

where

$$\chi_c=\chi_c'+i\chi_c''=i\chi_0''(1+\gamma^2)^{-1}, \tag{21a}$$

$$\chi_s^+=\chi_s'+i\chi_s''=\frac{\chi_0''[\beta(3\gamma^2-1-\beta^2)-i(1+\gamma^2)(\gamma^2-1-\beta^2)]}{(1+\gamma^2)[4\gamma^2+(\gamma^2-1-\beta^2)^2]}, \tag{21b}$$

$$\chi_s^-=-\chi_s'+i\chi_s'', \tag{21c}$$

$$\beta=\delta\tau>0. \tag{21d}$$

The saturating component of the field, F_c, is related to the corresponding frequency component of the polarization by χ_c. This quantity is unaffected by the sidebands and is the susceptibility of the medium in the presence of a monochromatic field of angular frequency ω_0.[2] The relationship of the sideband polarization components to the corresponding sidebands of the field can also be represented by susceptibilities which we have designated here as χ_s^+ (for the higher frequency sideband) and χ_s^- (for the lower frequency sideband). Using these susceptibilities, we can write, for the saturating component of the field,

$$\frac{1}{F_c^2}\frac{dF_c^2}{dz}=-\frac{4\pi\omega_0\chi_c''}{c}=-\frac{\alpha}{1+\gamma^2} \tag{22}$$

and for either sideband,

$$\frac{1}{F_s^2}\frac{dF_s^2}{dz}=-\frac{4\pi\omega_0\chi_s''}{c}=\frac{\alpha(\gamma^2-1-\beta^2)}{4\gamma^2+(\gamma^2-1-\beta^2)^2}. \tag{23}$$

When the equilibrium population distribution is unchanged by the radiation (γ^2 is negligible), the sideband susceptibilities χ_s^+ and χ_s^- vary with frequency according to the known linear dispersion properties of

the medium.[2] As the equilibrium is disturbed by the radiation field, these properties undergo a considerable change which can be illustrated by plotting the real and imaginary parts of χ_s^+ and χ_s^- as a function of $(\omega-\omega_0)\tau$ where ω represents the angular frequency of a sideband. The results are shown in Fig. 1 for a saturation parameter $\gamma^2=3$ for which $-\chi_s''$ has its maximum value. The linear absorption line is shown for comparison. The highest modulation frequency, δ_m, that will yield sideband amplification can be found from Fig. 1 and Eq. (21b) to be

$$\delta_m=(\gamma^2-1)^{1/2}\tau^{-1}. \tag{24a}$$

For a strongly saturated resonance corresponding to large values of γ^2 this result can be rewritten as

$$\delta_m\approx p_{12}F_c/\hbar. \tag{24b}$$

The term on the right-hand side of this equation represents the fluctuation frequency of the molecular transition probability[4] which, for a strongly saturated resonance, is equal to the power-broadened linewidth. Equation (24b) is, therefore, a statement of the fact that the sidebands can be amplified only over a frequency interval which is equal to the power-broadened linewidth.

We briefly note one more characteristic of the susceptibilities derived above. When a frequency component of the polarization does not vary linearly with the corresponding field component, the real and imaginary parts of the susceptibility do not satisfy the Kramers-Kronig relations.[5] This condition holds for the general form of the saturating component susceptibility, χ_c, but is not applicable to the sideband susceptibility functions, χ_s' and χ_s'', which can be shown to satisfy the Kramers-Kronig equations.

III. EXPERIMENTAL

Experimental studies were conducted by transmitting amplitude- and frequency-modulated fields through a waveguide containing hydrogen cyanide gas, $HC^{12}N^{15}$. The gas was contained at a pressure of[6] 2×10^{-2} mm Hg in a 20-ft-long, $\frac{3}{4}$-in.-i.d., circular copper waveguide operated in the TE_{01} mode.[7] The attenuation of electromagnetic energy in this mode due to wall losses was negligible compared to the effects of the gas. Transmission measurements showed that the total attenuation due to the evacuated waveguide was less than 0.2 dB.

Hydrogen cyanide was chosen for these experiments because it has a large electric dipole moment (3.0 D),[8] and, therefore, a large linear absorption coefficient. The isotopic form, $HC^{12}N^{15}$, was used because of the simplicity of its rotational spectrum. Since the quadrupole moment of each nucleus is zero, complications due to quadrupole hyperfine structure are avoided. The lower state of the observed transition is the lowest rotational state of the ground vibrational level and is specified by the rotational quantum numbers $J=0$, $m_J=0$. Choosing the direction of the linearly polarized electric field as the axis of quantization, the selection rule $\Delta m_J=0$ applies so that only one upper state ($J=1$, $m_J=0$) will be affected by the radiation.

Before a comparison can be made between theory and experiment, the free-space analysis presented above must be modified to account for the spatial variation of the electric field in the guide. In the Appendix the power attenuation or gain over the total guide length is computed for the individual frequency components of the radiation. The saturating component attenuation, P_c'/P_c (where P_c' represents the average output power and P_c the average input power), is evaluated as a function of two parameters: αL (L is the guide length) and the quantity $\gamma_m^2(0)$. The latter is the maximum value of the saturation parameter, γ^2, at the waveguide input and is proportional to the input power, P_c. Thus, the saturating component attenuation is determined by the linear attenuation (αL) and the degree of saturation at the input $[\gamma_m^2(0)]$.

Two types of experiments are described below. In the "slow modulation" experiments both AM and FM fields were used and the ratios P_c'/P_c and P_s'/P_s were measured as a function of the saturating component input power, P_c, for a fixed modulation frequency. In the "rapid modulation" experiments only AM fields were used and the sideband ratio P_s'/P_s was measured as a function of the modulation frequency for a fixed saturating component input power.

Slow Modulation

The slow modulation experiment was performed with the microwave circuit shown schematically in Fig. 2. A stabilized klystron generated the resonant frequency of the first rotational transition in the vibrational ground state of $HC^{12}N^{15}$ which was found to be[9]

$$\nu_0=(2\pi)^{-1}\omega_0=86\,055.0\pm0.3 \text{ Mc/sec}.$$

This monochromatic signal was transmitted through a variable attenuator to provide an adjustable saturating component with power, P_c. A side branch was used to phase shift and amplitude modulate this signal at the frequency, $\Delta\nu=70$ cps, to obtain the spectrum shown in circle I. The two branches were combined so that the resultant input spectrum shown in circle II corresponded to an amplitude or frequency modulated field. After transmission through the waveguide the output spectrum shown in circle III was combined with the homo-

[4] H. S. Snyder and P. I. Richards, Phys. Rev. **73**, 1178 (1948).
[5] A. M. Portis, Phys. Rev. **91**, 1071 (1953).
[6] This value was computed from our measurement of a collision-broadened linewidth, $(2\pi\tau)^{-1}$, of 0.5 Mc/sec and the $HC^{12}N^{14}$ data of A. G. Smith, W. Gordy, J. W. Simmons, and W. V. Smith, Phys. Rev. **75**, 260 (1949) relating linewidth to pressure. The estimated Doppler-broadening effects in our experiment were negligible.
[7] S. E. Miller, Bell System Tech. J. **33**, 1209 (1954).
[8] S. N. Ghosh, R. Trambarulo, and W. Gordy, J. Chem. Phys. **21**, 308 (1953).
[9] B. Senitzky and M. Piltch (to be published).

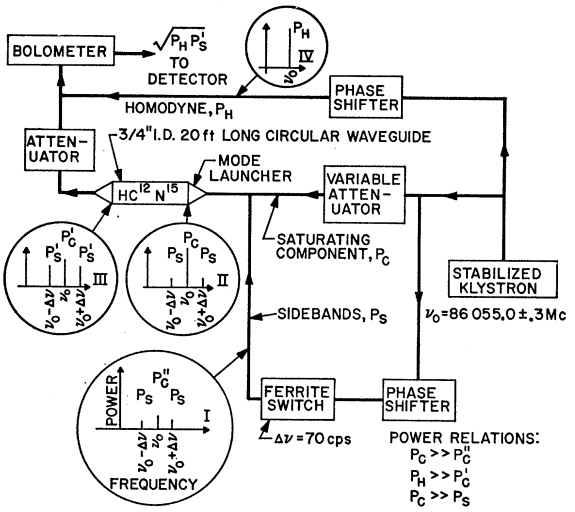

FIG. 2. Microwave circuit used to measure gain and attenuation. Frequency spectra for a sideband gain measurement are encircled.

dyne signal at the resonant frequency, ν_0, and the resultant millimeter-wave signal detected by a square-law bolometer. The phase of the homodyne signal was adjusted to maximize the amplitude of the 70-cps audio signal output from the bolometer which was proportional to $(P_H P_s')^{1/2}$. By evacuating the waveguide, a 70-cps signal proportional to $(P_H P_s)^{1/2}$ could be obtained. These signals were then used to determine the gain or attenuation, P_s'/P_s, of the sideband power.[10] Using this technique the sideband power ratio for amplitude modulation, P_s'/P_s(AM), the ratio for frequency modulation, P_s'/P_s(FM), and the saturating component ratio, P_c'/P_c, could be determined as a function of the relative input power.[11]

The experimental data were in agreement with the computations in the Appendix, as shown in Fig. 3 where the measured relative input power, P_c, was multiplied by an arbitrary constant to obtain the best fit to the theoretical curves. The latter were computed using the value of $\alpha L=6.0$,[12] which was found from the linear attenuation data $[\gamma_m^2(0)\rightarrow 0]$ in Fig. 3. The experimental values of the sideband power ratio for frequency modulation, P_s'/P_s(FM), coincided with the measured values of the saturating component ratio, P_c'/P_c, which are not shown in Fig. 3. These ratios remained less than unity as the resonance saturation increased. The measured sideband power ratio for amplitude modulation, P_s'/P_s(AM), behaved differently; it varied from an attenuation of -26 dB to a gain of 1.5 dB as the resonance saturation increased to a value corresponding to $\gamma_m^2(0)=10$. The behavior of this ratio for larger values of $\gamma_m^2(0)$ could be inferred from the theoretical curve which reaches a maximum at $\gamma_m^2(0)=10$ and then begins to decrease and asymptotically approach unity for larger values of $\gamma_m^2(0)$. The absolute value of the saturating component input power corresponding to $\gamma_m^2(0)=10$ was computed from Eq. (12) to be 4.8 mW, in agreement with an estimate based on a bolometer measurement.

Rapid Modulation

In a rapid amplitude modulation experiment we measured the sideband gain or attenuation as a function of modulation frequency for a fixed saturating component input power. Using a modified version of the microwave circuit shown in Fig. 2, measurements were made of (a) the fixed saturating component power ratio, P_c'/P_c; and (b) the variation of the sideband ratio, P_s'/P_s(AM), as a function of the modulation frequency, $\Delta\nu$. The experimental results are plotted in Fig. 4. The theoretical curve of P_s'/P_s(AM) vs $\Delta\nu$ can be plotted from Eq. (A5) provided the parameters αL, $\gamma_m^2(0)$, and τ are known. These were found from the unsaturated

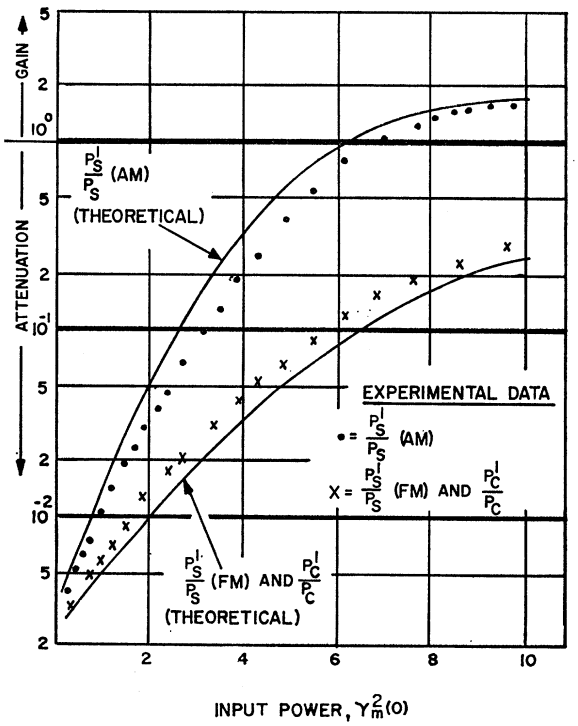

FIG. 3. Gain and attenuation characteristics showing the sideband power ratio for amplitude modulation, P_s'/P_s(AM), for frequency modulation, P_s'/P_s(FM), and saturating component ratio, P_c'/P_c, as a function of the normalized saturating component input power, $\gamma_m^2(0)$. The modulation frequency, $\Delta\nu$, is 70 cps and $\alpha L=6.0$.

[10] The bolometer audio output is actually a function of the power at *both* sideband frequencies, but since the attenuation or gain of the sidebands are equal, the measured ratio P_s'/P_s will apply to *either* sideband.

[11] Relative input power rather than absolute input power was measured because the bolometer used measured relative power with an accuracy of 2% whereas absolute power could only be estimated within a factor of 2.

[12] This value corresponds to an absorption coefficient of $\alpha=0.010$ cm^{-1} which can be compared to the value of 0.012 cm^{-1} computed from Eqs. (11) and (15).

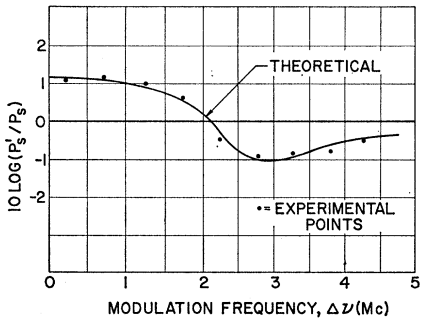

FIG. 4. Sideband power ratio for amplitude modulation, P_s'/P_s(AM), in decibels as a function of modulation frequency, $\Delta\nu$, for $\alpha L=5.25$, $(2\pi\tau)^{-1}=0.5$ Mc/sec, and $\gamma_m^2(0)=30$.

spectral line shape to be $(2\pi\tau)^{-1}=0.5$ Mc/sec and $\alpha L=5.25$. Using this value of αL and the measured ratio, P_c'/P_c, we could find $\gamma_m^2(0)=30$. The theoretical curve of P_s'/P_s(AM) vs $\Delta\nu$ was then plotted in Fig. 4 and is in agreement with the experimental data. As could be expected, the sideband power ratio, P_s'/P_s(AM), shown in Fig. 4 has the same frequency behavior as $-\chi_s''$ in Fig. 1.

IV. CONCLUSION

The theory and experiment described indicate that it is possible to use the nonlinear absorption properties of resonant media to transfer power from a strong saturating frequency component to weak sidebands. From a communications point of view, we can consider the saturating component as a local-oscillator signal and the weak sidebands as an incoming information signal. The use of higher frequency resonances is obviously desirable, since the amplification is proportional to the linear absorption coefficient, which increases rapidly with frequency. Another advantage of higher frequency operation is the feasibility of tuning a resonance by means of the Stark effect.

We are presently extending the investigation of this amplification process to resonant structures.

ACKNOWLEDGMENTS

We would like to thank M. Piltch and R. Olson for their technical assistance in this experiment. We also appreciate the encouragement of A. Feiner, J. Huss, and W. Bushunow of RADC during the course of this work.

APPENDIX. PROPAGATION IN WAVEGUIDE

The field in a circular waveguide which operates in a mode exhibiting azimuthal symmetry is a function of the distance from the axis, r, and the distance along the axis, z. We, therefore, rewrite Eq. (22) in the form

$$\frac{1}{F_c^2(r,z)}\frac{dF_c^2(r,z)}{dz}=-\frac{4\pi\omega_0\chi_c''(r,z)}{c}, \tag{A1}$$

where the difference between the propagation constant in free space and in the guide can be ignored for our experimental conditions. Letting

$$\gamma^2(r,z)=\gamma_m^2(z)(0.582)^{-2}J_1^2(3.83r/a), \tag{A2}$$

where a is the guide radius, J_1 is the first order Bessel function, and $\gamma_m(z)$ is the maximum value of the saturation parameter at a given propagation distance, z, Eq. (A1) can be integrated over the guide cross section to yield

$$\frac{1}{\gamma_m^2(z)}\frac{d\gamma_m^2(z)}{dz}=-\frac{4\pi\omega_0\bar{\chi}_c''(z)}{c}, \tag{A3}$$

where $\bar{\chi}_c''(z)$ is the averaged susceptibility,

$$\bar{\chi}_c''(z)=\int_0^a \chi_c''(r,z)J_1^2(3.83r/a)rdr \times\left[\int_0^a J_1^2(3.83r/a)rdr\right]^{-1}.$$

Equation (A3) can be numerically solved for the power attenuation at a given distance, z.

$$P_c(z)/P_c(0)=\gamma_m^2(z)/\gamma_m^2(0), \tag{A4}$$

and can be expressed as a function of two parameters, αz and $\gamma_m^2(0)$. For convenience in notation, the attenuation over the total guide length, L, will be written in the form

$$P_c(L)/P_c(0)=P_c'/P_c.$$

The sideband power gain or attenuation can be computed numerically from

$$P_s'/P_s=\exp\left\{-\left[4\pi\omega_0/c\int_0^L\int_0^a \chi_s''(r,z)J_1^2(3.83r/a)rdrdz\right]\times\left[\int_0^a J_1^2(3.83r/a)rdr\right]^{-1}\right\}, \tag{A5}$$

and can then be expressed as a function of the three parameters αL, $\gamma_m^2(0)$, and β^2.